ORIGINAL RESEARCH PAPER

Research on human gait prediction and recognition algorithm of lower limb-assisted exoskeleton robot

Tao Qin[1] · Yong Yang[1] · Bin Wen[2] · Zhengxiang Chen[1] · Zhong Bao[1] · Hao Dong[1] · Ke Dou[1] · Changmao Yang[1]

Abstract

Wearable lower limb-assisted exoskeleton robot can improve a human's ability to walk long distances under heavy load. Accurate perception and recognition of human lower limb motion and real-time input of exoskeleton control system parameters have always been the key technologies of wearing lower limb assist exoskeleton robot. To solve the problem of poor real-time and stability of the lower extremity exoskeleton system caused by time delay in transmitting gait information from the lower extremity assisted exoskeleton robot perception system to the control system, we proposed a new human gait prediction and recognition algorithm. Based on the gait sample data of human lower limbs, we proposed a prediction algorithm concerning least-squares support vector regression (LS-SVR) to predict the gait data at the next moment of human lower limbs movement. We proposed a human gait phase recognition algorithm using fuzzy theory to identify the gait phase at the next moment of human lower limb movement. The proposed algorithm can identify the heel landing phase, the load-supporting phase, the pre-swing phase, and the swing phase of human lower limbs. Experimental results demonstrate that gait prediction accuracy is 99.83% and the gait phase recognition rate based on the predicted gait data of 120 complete gait cycles is 99.93%. It comes up to a feasible method for wearable lower limb-assisted exoskeleton robot intelligent perception technology. New algorithms improve the recognition rate of gait phase prediction and effectively improve the real-time, stability, and robustness of the lower extremity exoskeleton robot system. The proposed gait prediction and recognition model can help gait recognition tasks to overcome the difficulties in real application scenarios and provide a feasible method for a lower extremity assisted exoskeleton robot perception system.

Keywords Exoskeleton robot · LS-SVR · Fuzzy theory · Gait data prediction · Gait phase recognition

1 Introduction

The exoskeleton robot is a perfect combination of human "intelligence" and machine "physical ability" [1]. It can complete all kinds of assistance work submitting to the human mind [2]. The concept of the exoskeleton robot was proposed by the military in the early 2000s in the hope of improving the individual combat capability of soldiers, increasing military mobility and combat effectiveness, and improving national defense capabilities. At present, the lower limb-assisted exoskeleton robot is mainly used to help the

elderly walk and soldiers march long distances. With the development of assisted exoskeleton technology, assisted exoskeleton robot is gradually applied in daily life. In many application scenarios, it has shown super high standards and taken many advantages to human life. For example, lower extremity rehabilitation exoskeleton helps patients recover, and lower extremity power exoskeleton helps soldiers march for long distances [3].

Most researchers have focused attention on human gait recognition for lower extremity assisted exoskeleton robot. Luo and Tjahjadi [4] proposed that 3D Gait Semantic Folding based on Hierarchical Temporal Memory (HTM) was applied to recognize and understand gait. They used a realistic 3-dimensional(3D) human structural data and sequential pattern learning framework with top-down attention modulating mechanism based on HTM to address unstructured data problems: multi-views, occlusion, clothes, and object carrying conditions from images and videos. By this

✉ Tao Qin
  pfmzlio@163.com

1 Yichang Testing Technique Research Institute, Yichang, China

2 China Three Gorges University, Yichang, China

model, they obtained a perfect performance gain in terms of accuracy and robustness. Davarzani et al. [5] utilized wearable soft robotic sensors (SRS) to perceive the foot–ankle basic movement during gait cycles of eight gait phases. Using multi-variable linear regression, an artificial neural network (ANN), and a time-series long short-term memory (LSTM) network, they quantify the performance between SRS datasets and three-dimensional (3D) motion capture datasets. Therefore, they verified the high performance of SRS in capturing foot–ankle kinematics during human gait cycle. The experiment results demonstrated there was little difference between the error rate of the various models. Ait O. Lishani et al. [6] proposed an approach to recognize human gait based on local multi-scale feature descriptors in the Gait Energy Image (GEI). The novel proposed method was a fusion of multi-scale Local Binary Pattern (MLBP) and Gabor filter bank to extract human gait features. Spectra Regression Kernel Discriminant Analysis (SRKDA) reduction algorithm was applied to reduce gait data dimensions. They used CASIA and USF Gait databases to conduct the experiments and achieve better recognition performances up to 92%. Akhil et al. [7] made use of the ratio of hip, knee and ankle joints as the primary input parameters for the control system of a rehabilitation exoskeleton. By analyzing two-dimension features of human gait, they determined that human gait characteristics can be obtained as the ratio of the hip to knee, knee to ankle, hip to the ankle, and the time taken for achieving a gait.

By analyzing human gait recognition's current research status, gait recognition features are extracted from videos and pictures of human movement. The human gait feature extraction method has the defection of incomplete extraction of human gait details, reducing gait recognition accuracy. Besides, the prediction of human gait information is relatively rare. To improve the real-time and accuracy of the input parameters of the control system of the lower limb exoskeleton robot, our study mainly focuses on predicting gait phases by gait sample data from human lower extremities. By inputting the gait phase of the next moment in advance, the system's delay error can be reduced. The new gait recognition method can improve the stability and comfort of the rehabilitation exoskeleton.

In this study, the lower extremity assisted exoskeleton robot's sensing system senses the motion state information of human lower extremity through sensors. It mainly senses the gait information of the human lower limb movement. After preprocessing the data detected by multiple sensors, a feature fusion algorithm is used to extract the gait characteristics and identify the human lower limb movement's gait phase. The main gait phases of lower limbs are the heel landing phase, load-supporting phase, pre-swing phase, and swing phase. The input parameters of the lower limb-assisted exoskeleton robot control system are the gait phase

recognized by the sensory system. Therefore, real-time and accurate gait phase perception can significantly improve the assisted exoskeleton robot's control accuracy and system reliability. The perception system of assisted exoskeleton robots can perceive the gait information of human lower limbs, so that the mechanical skeleton can follow the movement state of human lower limbs. In following the motion state of human lower limbs, the motion state of assisted exoskeleton robot lags the motion state of the human body due to the time delay and lag in gait recognition and transmission by the sensory system. It seriously affects the stability and reliability of the exoskeleton robot control system.

Therefore, this paper has proposed an improved gait prediction algorithm based on least-squares support vector regression to predict the gait data of the human body at the next moment, and has combined the gait recognition algorithm based on fuzzy theory to identify the gait phases. At the same time of recognizing the current gait, the predicted gait phase is inputted into the control system. The control system could make a real-time control strategy to improve the reliability and stability of the lower limb.

assisted exoskeleton robot system. Figure 1 is the structure simulation of the lower extremity assisted exoskeleton robot. Each major part of the diagram is marked with a character. "a", "b", "e" and "h" stand for motors that drive the joint movement of the exoskeleton robot. The "c" and "d" are gait signal processor hardware systems. The "f", "g", "i"
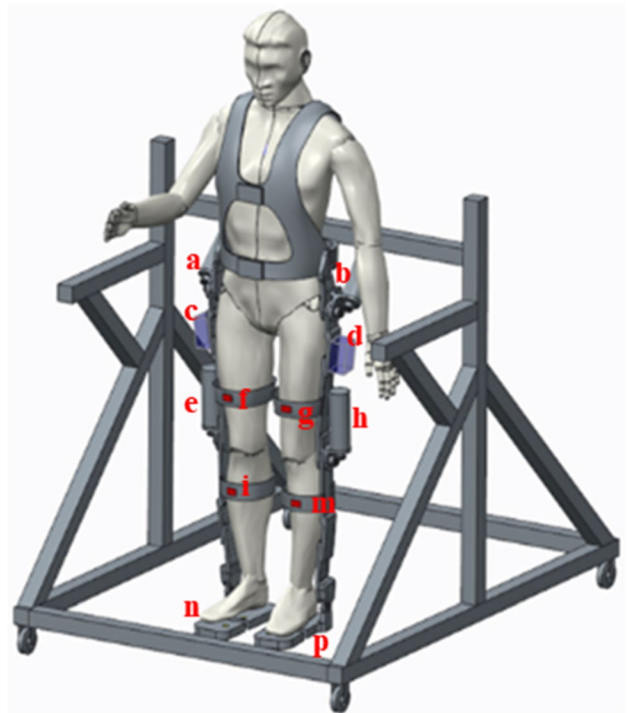
Fig. 1 Structure simulation of lower extremity assisted exoskeleton robot

and "m" are Nine-axis inertial sensors, whose major task is detection of changes in hip and knee angles. The "n" and "p" represent a set of pressure sensors mounted on the right and left feet, respectively. Each set contains four pressure sensors.

The rest of this paper includes four sections. Section 1 demonstrates the acquisition method for original data of gait and analyzes the related rule of gait data. Section 2 describes the proposed method that least-squares support vector regression (LS-SVR) is utilized to predict human gait data. Section 3 introduces the process for the recognition of four gait phases based on the fuzzy theory. In Sect. 4, the results of the proposed algorithms are analyzed. The gait phase prediction algorithm based on the Kalman algorithm is selected to compare with the proposed gait phase prediction algorithm. Section 5 concludes the entire paper.

2 Gait data perception and analysis of lower limbs

By sensing the change of plantar pressure when the human body is in motion, the exoskeleton sense system can effectively identify the human body's motion state. According to the law of the pressure change at different positions of the bottom of the foot when the bottom of the human body is in motion, the pressure at the four positions of the bottom of the human body is mainly collected to analyze the motion state of the human body [8]. Figure 2 shows the division of the plantar region of the right foot. Besides, the left foot has the same plantar region as the right foot. The "$Pressure\ transducer\ A_1$" and "$Pressure\ transducer\ A_2$" are installed in the T1 regions of the left and right feet to detect changes of signals in T1 regions. The "$Pressure\ transducer\ B_1$" and "$Pressure\ transducer\ B_2$" are installed in the junction of M2 and M3 regions of the left and right feet, respectively, to detect.

Changes of signals in these regions. The "$Pressure\ transducer\ C_1$" and "$Pressure\ transducer\ C_2$" are installed in the LM regions of the left and right feet to detect changes of signals in the LM regions. At the junction of HL and HM, "$Pressure\ transducer\ D_1$" and "$Pressure\ transducer\ D_2$" are installed to detect signal changes of the left and right feet, respectively.

The four locations to perceive plantar pressure are the junction of T1, M2 and M3, LM, HL and HM [9–11]. The four plantar positions correspond to four groups of pressure sensors A, B, C, and D. The changes of gait signal of the feet under the uniform walking speed of 1.5 m/s are detected by the assisted exoskeleton robot perception system as the sample data. The data used in this project are gait data collected in the experiment of lower limb movement. The data sample size is 7200 sample points with 120 complete gaits. Figures 3 and 4 are sample figures of the gait data of the pretreated plantar pressure.

Figures 3 and 4 show the pressure variation curves of four complete gait cycles at different left and right plantar positions during uniform walking. Through the plantar pressure sensor, the pressure signal is converted into a voltage signal. The pressure variation range of Fig. 2 is between [0 1.7], and that of Fig. 4 is between [0 1.1]. The data of a complete cycle within [0 1.5] seconds in Fig. 4 are selected for analysis, and the gait data of four groups of foot pressure under uniform walking state presented periodicity. The variation trends of the four curves increase first and then decrease. The left and right plantar pressure changes alternately, and the movement rules are like the same change period.
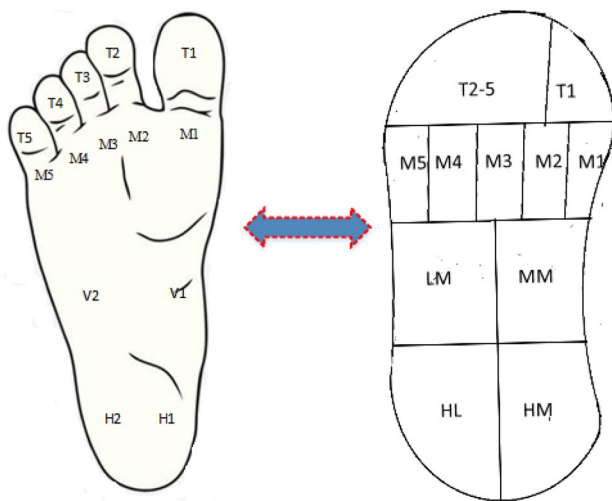

**Fig. 2** Plantar region division diagram

3 Human gait data prediction algorithm model based on LS-SVR

This study proposes an algorithm for human gait data prediction based on least square support vector regression. Basing on the gait sample information obtained by the assisted exoskeleton robot perception system, the gait data prediction algorithm based on LS-SVR predict gait data of human motion state at the next moment or several moments. According to the foot pressure gait data analysis in the first section, the left lower limb, and the right lower limb has similar motion states. Therefore, the left lower limb is selected as the research object. Gait data of the left lower limb are selected as training samples.

Fig. 3 Original pressure data of left foot
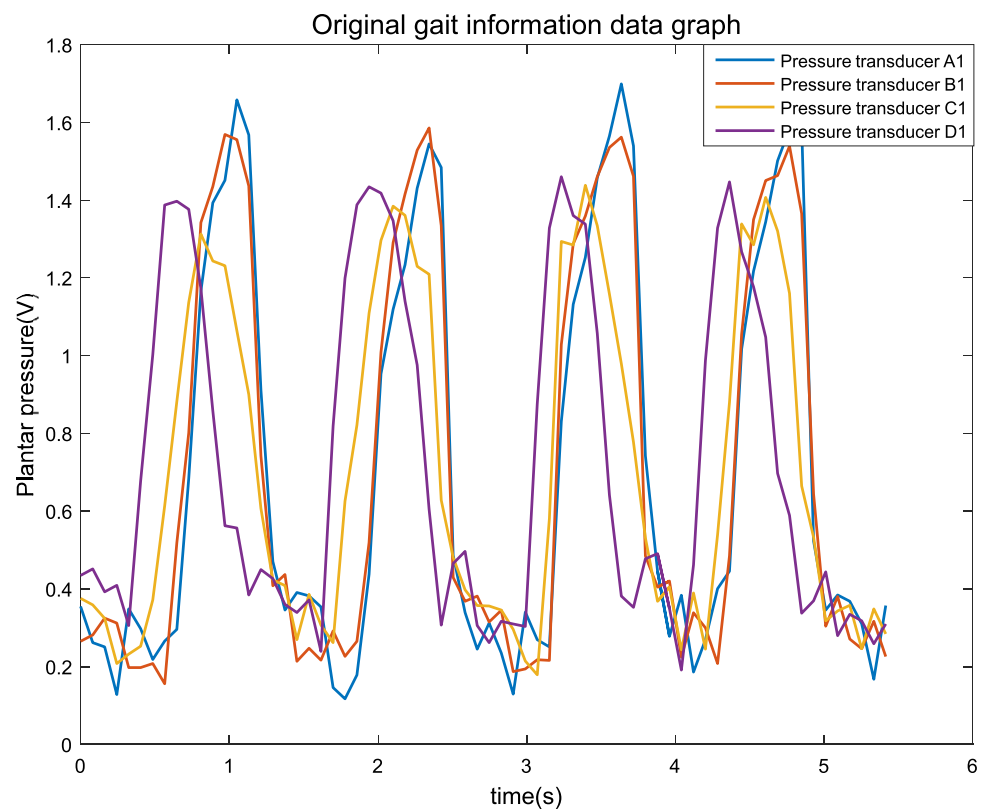
Fig. 4 Original pressure data of right foot
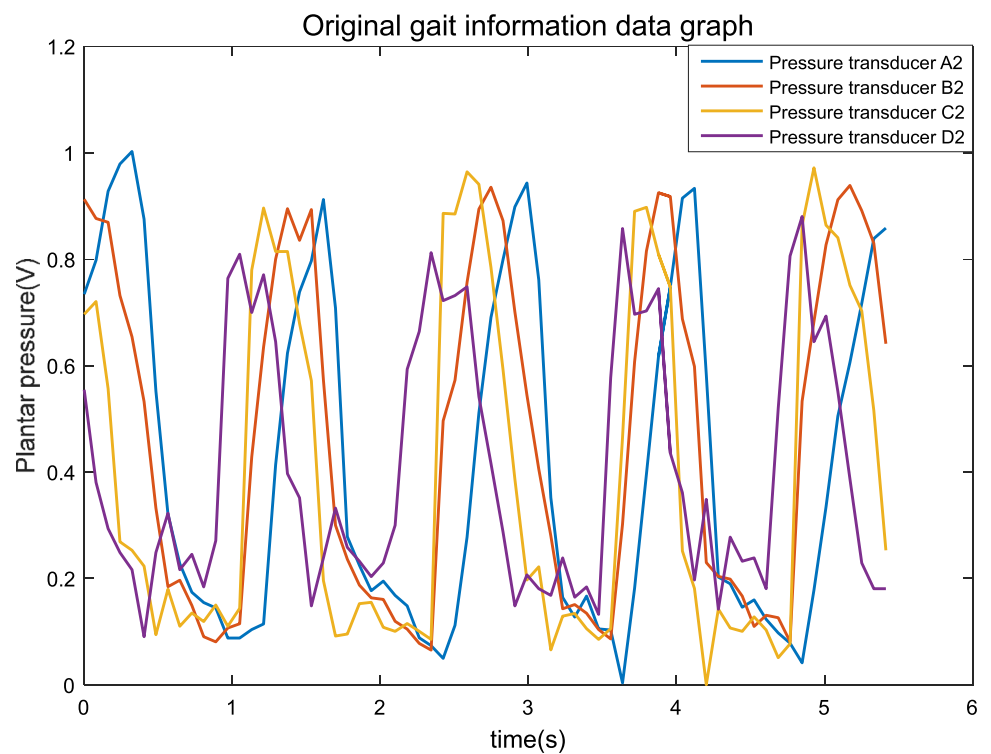
3.1 Gait prediction algorithm model

The distribution of gait sample data of lower limbs is nonlinear and cannot be effectively classified by linear support vector machine in low-dimensional space. A nonlinear support vector machine model is proposed to transform nonlinear problems into linear problems in this article. The training samples are mapped from the low-dimensional space to the high-dimensional space using a kernel function to make samples more easily separable [12].

Let $\varphi(x)$ represents the eigenvector of the mapped x. Therefore, in the feature space, the model corresponding to the partition hyperplane can be expressed as,

$$f(x) = w^T \varphi(x) + b \qquad (1)$$

Then there is the minimization function,

$$\frac{1}{2} \min_{w,b} \|w\|^2$$
$$s.t: \ y_i \left(w^T \varphi(x_i) + b \right) \geq 1 \quad (i = 1, 2, 3, ..., m) \qquad (2)$$

Its dual problem is,

$$\max_a \sum_{m=i}^{m} a_i - \frac{1}{2} \sum_{i=1}^{m} \sum_{j=1}^{m} a_i a_j y_i y_j \varphi(x_i)^T \varphi(x_j)$$
$$s.t. \ \sum_{i=1}^{m} a_i y_i = 0, \ a_i \geq 0, \ i = 1, 2, 3, ..., m \qquad (3)$$

when solving Eq. (3), we first need to calculate $\varphi(x_i)^T \varphi(x_j)$. $\varphi(x_i)^T \varphi(x_j)$ is the inner product of samples x_i and x_j mapped to the eigenspace. Because the dimension of the eigenspace can be high, it is often difficult to compute $\varphi(x_i)^T \varphi(x_j)$ directly. We use Eq. (4) to simplify this.

$$k(x_i, x_j) \leq \varphi(x_i), \varphi(x_j)^T \geq \varphi(x_i)^T \varphi(x_j) \qquad (4)$$

The inner product of x_i and x_j in the eigenspace is equal to what they calculated in their original sample space by the function $k(x_i, x_j)$[13]. Therefore, Eq. (3) can be expressed as Eq. (5).

$$\left\{ \begin{array}{l} \max_a \sum_{m=i}^{m} a_i - \frac{1}{2} \sum_{i=1}^{m} \sum_{j=1}^{m} a_i a_j y_i y_j k(x_i, x_j) \\ s.t. \ \sum_{i=1}^{m} a_i y_i = 0, \ a_i \geq 0, \ i = 1, 2, 3, ..., m \end{array} \right\} \qquad (5)$$

We obtain Eq. (6) by solving Eq. (5).

$$f(x) = w^T \varphi(x) + b$$
$$= \sum_{i=1}^{m} a_i y_i \varphi(x_i)^T \varphi(x_j) + b \qquad (6)$$
$$= \sum_{i=1}^{m} a_i y_i k(x_i, y_i) + b$$

In Eq. (6), $k(x_i, y_i)$ is a Gaussian kernel function. When linear indivisible samples are classified in the model, some sample points (x_i, y_i) cannot meet the condition of higher than or equal to 1, and the sample points fall between the hyperplane and the boundary. Therefore, a relaxation variable $\varepsilon_i \geq 0$ can be introduced for each sample point, so that the result that an interval is applied to the relaxation variable is greater than or equal to 1, so that constraints are translated into Eq. (7).

$$y_i \left(w^T x + b \right) \geq 1 - \varepsilon_i \qquad (7)$$

Meanwhile, for each relaxation variable $\varepsilon_i \geq 0$, the objective function becomes Eq. (8).

$$\min_{w,b,\varepsilon_i} \frac{1}{2} \|w\|^2 + C \sum_{i=1}^{m} \varepsilon_i \qquad (8)$$

$C > 0$ is the penalty factor. When the value of C is large, the penalty for misclassification increases [14, 15]. At this point, the linear problem is transformed into a convex quadratic programming problem again and solved.

$$\frac{1}{2} \min_{w,b} \|w\|^2 + C \sum_{i=1}^{m} \varepsilon_i$$
$$s.t: \ y_i \left(w^T x_i + b \right) \geq 1 - \varepsilon_i \qquad (9)$$
$$(i = 1, 2, 3, ..., m)$$

It turns into a dual problem. Its Lagrangian function is Eq. (10).

$$L(w, b, a, \varepsilon, \mu) = \frac{1}{2} \|w\|^2 + C \sum_{i=1}^{m} \varepsilon_i - \sum_{i=1}^{m} \mu_i \varepsilon_i$$
$$+ \sum_{i=1}^{m} a_i \left(1 - \varepsilon_i - y_i \left(w^T x_i + b \right) \right) \qquad (10)$$

In Eq. (10), $\varepsilon_i \geq 0$ and $\mu_i \geq 0$ are Lagrange multipliers. Let $L(w, b, a, \varepsilon, \mu) = 0$, after partial derivatives of w, b and ε are obtained, respectively, Eq. (11) is the result of the conversion.

$$\left\{ \begin{array}{l} w = \sum_{i=1}^{m} a_i y_i x_i \\ \sum_{i=1}^{m} a_i y_i = 0 \\ C = a_i + u_i \end{array} \right. \qquad (11)$$

Equation (12) is calculated by substituting Eq. (11) into Eq. (10).

$$
\begin{aligned}
&\max \sum_{m=i}^{m} a_i - \frac{1}{2} \sum_{i=1}^{m} \sum_{j=1}^{m} a_i a_j y_i y_j x_i x_j \\
&s.t : \sum_{i=1}^{m} a_i y_i = 0 \\
&\quad a_i \geq 0, \mu_i \geq 0 \\
&\quad i = 1, 2, 3, ..., m \\
&\quad C = a_i + \mu_i
\end{aligned}
\tag{12}
$$

According to the above Equation, the parameters are calculated, and the mathematical model is finally obtained, as shown in Eq. (13).

$$
f(x) = \left(w^T x + b\right) = \sum_{i=1}^{m} a_i y_i x_i^T x + b
\tag{13}
$$

The constraint condition of Eq. (13) is Eq. (14).

$$
\begin{cases}
a_i \geq 0 \\
y_i f(x_i) \geq 1 - \varepsilon_i \\
a_i \left(y_i f(x_i) - 1 + \varepsilon_i \right) = 0 \\
\varepsilon_i \geq 0, \ \mu_i \varepsilon_i = 0
\end{cases}
\tag{14}
$$

3.2 Improved least squares support vector machine regression algorithm

The derivation of the above equations indicates that the support vector machine utilizes the Lagrange multiplier to solve a, which requires a lot of computation. However, the need of the exoskeleton robot perception system is to quickly and timely perceive the motion state of human lower limbs. Therefore, the support vector machine cannot meet lower extremity assisted exoskeleton robots' demand when predicting the human lower extremity motion state. Combining the advantages of least square method and support vector

machine, the algorithm is improved [16]. The model of the improved prediction algorithm is shown in Eq. (15).

$$
\begin{aligned}
&\frac{1}{2} \min_{w,b} \|w\|^2 + C \sum_{i=1}^{m} \varepsilon_i \\
&s.t. \ y_i \left(w^T x_i + b \right) = 1 - \varepsilon_i (i = 1, 2, 3, \ldots, m)
\end{aligned}
\tag{15}
$$

Compared with the support vector machine model, the constraints of the model of least-squares support vector machine become equations, which reduces the computation of the model.

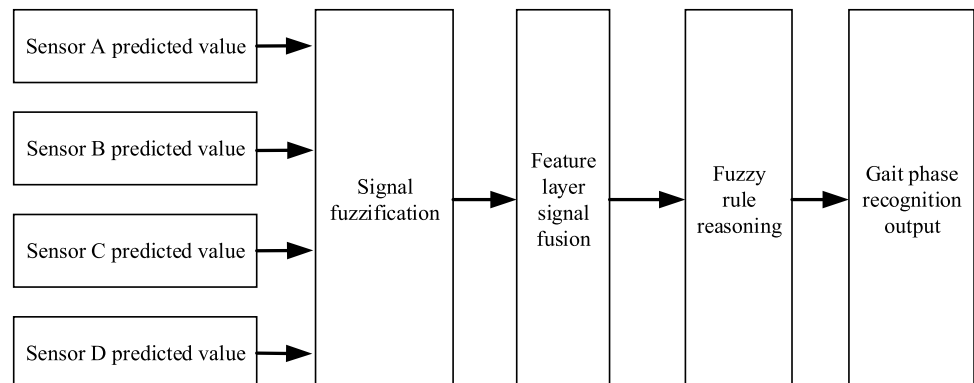## 4 Gait phase recognition algorithm based on fuzzy theory

The flow of lower limb gait phase recognition algorithm based on fuzzy theory algorithm is shown in Fig. 5. The gait phase recognition algorithm realizes the process of fuzzification [17], feature layer fusion, fuzzy rule inference, and gait phase output of four groups of gait prediction data: "*Forcast data A_1*", "*Forcast data B_1*", "*Forcast data C_1*" and "*Forcast data D_1*".

4.1 Fuzzy gait prediction data

Selecting the appropriate fuzzy set and membership function is the basis of accurately fuzzy the gait data predicted by the least-squares support vector regression algorithm [18, 19]. The distribution range of the predicted values of the four groups of gait data is all between [0 2]. Thus, the fuzzy sets are determined as "0" and "1". A fuzzy membership function is designed to divide the interval between "0" and "1" gait prediction data in [0 2]. The membership function of Eq. (16) is adopted.

$$
f^{L\arg e}(p) = \frac{1}{1 + e^{-s(p - pinv)}}
\tag{16}
$$

Fig. 5 Flow chart of gait phase recognition algorithm based on fuzzy theory

Sensor A predicted value → Sensor B predicted value → Sensor C predicted value → Sensor D predicted value → Signal fuzzification → Feature layer signal fusion → Fuzzy rule reasoning → Gait phase recognition output

where p represents the predicted gait data value and *pinv* represents the threshold value [20]. The threshold is determined by analyzing the variation trend of the gait data prediction curve. The prediction curves of gait are all periodic. The predicted gait values in a period increase first and then decrease successively on the time axis. This change rule can also be analyzed from Fig. 10. The four curves will intersect and divide a full gait cycle into several subintervals. Each subinterval has a curve segment with a higher value than the other three. The value of *pinv* can be obtained by analyzing the intersection value of four gait prediction curves. *S* is the sensitivity coefficient, and the size is generally 10 [21]. The fuzzy sets of the predicted gait data are divided into "1" and "0" states. "1" means that the predicted value of the gait data of the pressure sensor is valid, and "0" means that the predicted value of the gait data of the pressure sensor is invalid. Therefore, after the parameter values of the fuzzy membership function in Eq. (16) are determined, the fuzzification of the predicted gait data can be completed.

When Eq. (17) is true, the fuzzy value is "0", which indicates that the predicted gait data value at the current moment is invalid, or that the pressure sensor does not detect the plantar pressure signal at the next moment [22].
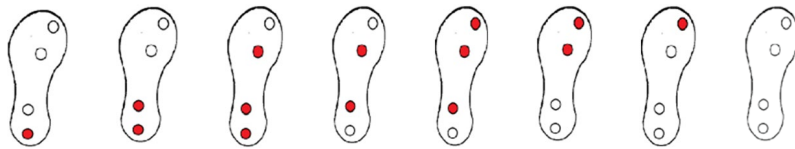
$$f^{\text{Large}}(p) \in [0, 0.5] \ or \ p < \text{pinv}, \tag{17}$$

when Eq. (18) holds, the fuzzy value is defined as "1", indicating that the predicted gait data value at the current moment is an effective value, and that the pressure sensor detects the pressure signal at the bottom of the foot at the next moment.

$$f^{\text{Large}}(p) \in (0.5, 1] \ or \ p > \text{pinv} \tag{18}$$

The four groups of gait predicted data are fuzzy by a membership function. Above completes the first important part of the gait phase recognition algorithm based on fuzzy theory.

4.2 Information fusion at feature layer

After the fuzzing of the four groups of gait's predicted data, according to the characteristics of the four gait phases of the human lower limb motion state [23], the feature layer information fusion is realized fuzzy rule table is designed. The fuzzy rule table design principle divides four groups of gait prediction data into eight states, which is based on the theory of gait cycle division during lower limb walking. There are two gait states of heel landing, three gait states of load support, two gait states of pre-swing and one gait state of swing.

In Table 1, in the fuzzy rule table based on gait phase analysis, FDA, FDB, FDC and FDD are the predicted values of gait data installed in pressure sensors at corresponding positions on the bottom of the foot. The Gait Phase stands for GP, GP1 for heel down Gait Phase, GP2 for load support Gait Phase, GP3 for pre-swing Gait Phase, and GP4 for swing Gait Phase.

4.3 Fuzzy rule reasoning

Using the Larsen product suggestion method as an inference operator, the rules in Table 2 are transformed into mathematical expressions. The following four equations show the mathematical expression for the heel landing phase, the load-supporting phase, the pre-swing phase and the swing phase. For instance, by querying Table1, there are two types of reasoning about GP1. Equation (19) describes the reasoning process of GP1. $f(p_{V_{FDA}}), f(p_{V_{FDB}}), f(p_{V_{FDC}})$ and $f(p_{V_{FDD}})$ stand for the fuzzy inference values of A, B, C, D.

Table 2 Gait data prediction results analysis table

Indicators Point estimate	Error range	Minimum RMS error	Accuracy
Forecast data A_1	[−0.0397 0.0390]	0.0160	99.89%
Forecast data B_1	[−0.0496 0.0548]	0.0242	99.85%
Forecast data C_1	[−0.0514 0.0503]	0.0252	99.67%
Forecast data D_1	[−0.0393 0.0360]	0.0177	99.93%

Table 1 Fuzzy rule table based on gait phase analysis

State division Fuzzy symbol								
FDA	0	0	0	0	1	1	1	0
FDB	0	0	1	1	1	1	0	0
FDC	0	1	1	1	1	0	0	0
FDD	1	1	1	0	0	0	0	0
GP	GP1	GP1	GP2	GP2	GP2	GP3	GP3	GP4

$f^{Small}(p_{V_{FDA}}) \to 0$ illustrates that the fuzzy inference value of sensor A is "0". $f^{L\arg e}(p_{V_{FDA}}) \to 1$ states that the fuzzy inference value of sensor A is "1". Value of GP1 can be obtained by fusion of fuzzy values of sensors A, B, C and D. When $f^{Small}(p_{V_{FDA}}) \to 0, f^{Small}(p_{V_{FDB}}) \to 0, \; f^{Small}(p_{V_{FDC}}) \to 0$ and $f^{L\arg e}(p_{V_{FDD}}) \to 1$, it illustrates that the gait phase is the heel landing phase. When $f^{Small}(p_{V_{FDA}}) \to 0, f^{Small}(p_{V_{FDB}}) \to 0,$ $f^{L\arg e}(p_{V_{FDC}}) \to 1$ and $f^{L\arg e}(p_{V_{FDD}}) \to 1$, it also is the heel landing phase. GP2, GP3 and GP4 can be interpreted in the same manner.

Figures 6, 7, 8, 9 and 10 are gait data prediction graphs of "$Pressure\ transducer\ A_1$", "$Pressure\ transducer\ B_1$", "$Pressure\ transducer\ C_1$" and "$Pressure\ transducer\ D_1$" based on least-squares support vector regression algorithm, respectively. In each image is a four-cycle gait data prediction."$Original\ data\ A_1$", "$Original\ data\ B_1$", "$Original\ data\ C_1$" and "$Original\ data\ D_1$" respectively, represent the sample values of the left foot pressure sensors A_1, B_1, C_1 and D_1, while "$Forecast\ data\ A_1$", "$Forecast\ data\ B_1$", "$Forecast\ data\ C_1$" and "$Forecast\ data\ D_1$" represent the pre-

$$\left.\begin{array}{l} (f^{Small}(p_{V_{FDA}}) \to 0) \times (f^{Small}(p_{V_{FDB}}) \to 0) \times (f^{Small}(p_{V_{FDC}}) \to 0) \times (f^{L\arg e}(p_{V_{FDD}}) \to 1) \\ (f^{Small}(p_{V_{FDA}}) \to 0) \times (f^{Small}(p_{V_{FDB}}) \to 0) \times (f^{L\arg e}(p_{V_{FDC}}) \to 1) \times (f^{L\arg e}(p_{V_{FDD}}) \to 1) \end{array}\right\} = \mu_{GP1} \to 1 \qquad (19)$$

$$\left.\begin{array}{l} (f^{Small}(p_{V_{FDA}}) \to 0) \times (f^{L\arg e}(p_{V_{FDB}}) \to 1) \times (f^{L\arg e}(p_{V_{FDC}}) \to 1) \times (f^{L\arg e}(p_{V_{FDD}}) \to 1) \\ (f^{Small}(p_{V_{FDA}}) \to 0) \times (f^{L\arg e}(p_{V_{FDB}}) \to 1) \times (f^{L\arg e}(p_{V_{FDC}}) \to 1) \times (f^{Small}(p_{V_{FDD}}) \to 0) \\ (f^{L\arg e}(p_{V_{FDA}}) \to 1) \times (f^{L\arg e}(p_{V_{FDB}}) \to 1) \times (f^{L\arg e}(p_{V_{FDC}}) \to 1) \times (f^{Small}(p_{V_{FDD}}) \to 0) \end{array}\right\} = \mu_{GP2} \to 1 \qquad (20)$$

$$\left.\begin{array}{l} (f^{L\arg e}(p_{V_{FDA}}) \to 1) \times (f^{L\arg e}(p_{V_{FDB}}) \to 1) \times (f^{Small}(p_{V_{FDC}}) \to 0) \times (f^{Small}(p_{V_{FDD}}) \to 0) \\ (f^{L\arg e}(p_{V_{FDA}}) \to 1) \times (f^{Small}(p_{V_{FDB}}) \to 0) \times (f^{Small}(p_{V_{FDC}}) \to 0) \times (f^{Small}(p_{V_{FDD}}) \to 0) \end{array}\right\} = \mu_{GP3} \to 1 \qquad (21)$$

$$(f^{L\arg e}(p_{V_{FDA}}) \to 0) \times (f^{Small}(p_{V_{FDB}}) \to 0) \times (f^{Small}(p_{V_{FDC}}) \to 0) \times (f^{Small}(p_{V_{FDD}}) \to 0) = \mu_{GP4} \to 1 \qquad (22)$$

5 Analysis of experimental results

5.1 Analysis of gait data prediction results

The improved gait data prediction algorithm based on the least square support vector regression utilizes 120 complete gait data of human lower limbs as training samples. The predictive algorithm model has two parameters γ and C. γ is the coefficient of the Gaussian kernel function.C represents the penalty factor, and the larger C represents the smaller the allowable model error rate[24]. Proper parameters γ and C can minimize the error between the predicted gait data and the test data. The model parameters of gait prediction algorithm proposed in this paper are shown in Eq. (23). The values of parameters γ and C are obtained by manually adjusting parameters in the experiment.

$$\begin{array}{ll} \gamma_1 = 0.015 & C_1 = 340 \\ \gamma_2 = 0.015 & C_2 = 323 \\ \gamma_3 = 0.015 & C_3 = 353 \\ \gamma_4 = 0.015 & C_4 = 289 \end{array} \qquad (23)$$

dicted values of gait data. "$error$" are the error curves of gait sample data and gait prediction data. To demonstrate the effectiveness of the proposed gait prediction algorithm, the gait prediction curves of the four sensors are shown in Fig. 10. Compared with the gait sample curves in Fig. 3, the predicted gait curves maintain same variation pattern as the original gait curves, but they are smoother.

The proposed gait prediction algorithm's effectiveness is verified from three aspects: error range, minimum RMS error, and accuracy. Table 2 shows the analysis of gait data prediction results. Table 2 indicates that the error range and minimum RMS error of the four gait prediction curves are all within the acceptable range. The prediction accuracy is more than 99.6%.

5.2 Gait phase output analysis

The left foot's output is the heel landing phase, the load support phase, the pre-swing phase, and the swing phase. Figure 11 shows the gait phase prediction diagram of four complete cycles within (0, 5.4136) seconds.

On the longitudinal axis ("Gait Phase"), "1" stands for the heel landing phase, "2" stands for the load-supporting
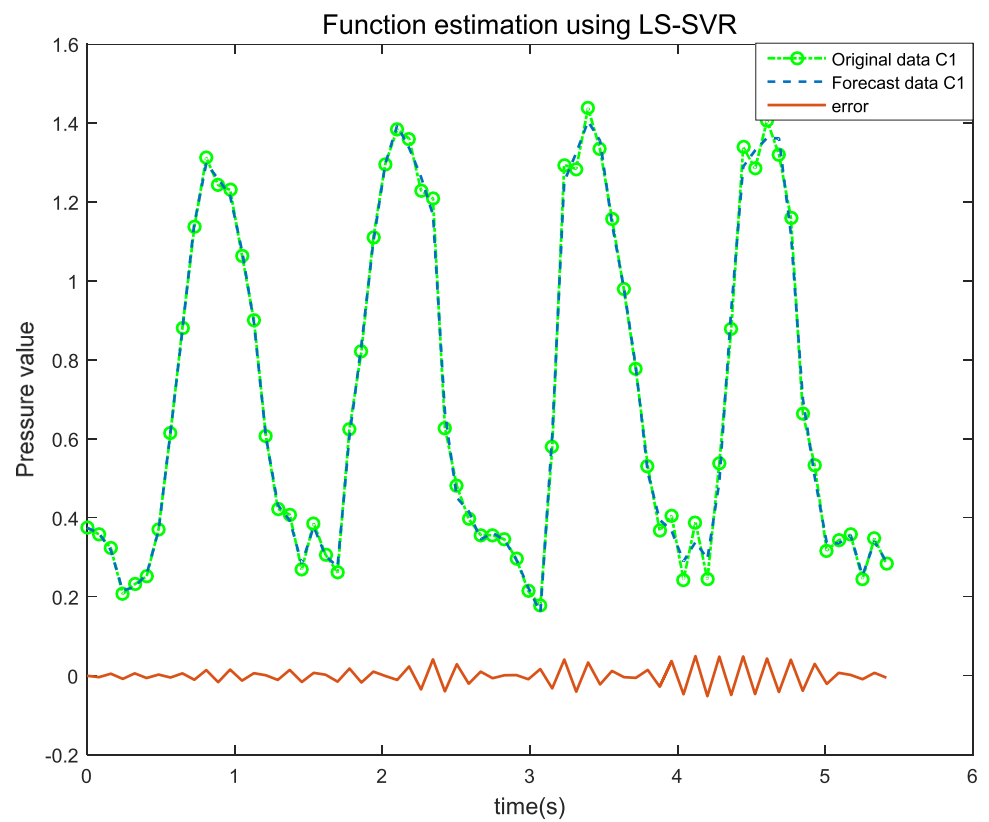
Fig. 6 A_1 prediction of sensor sample data
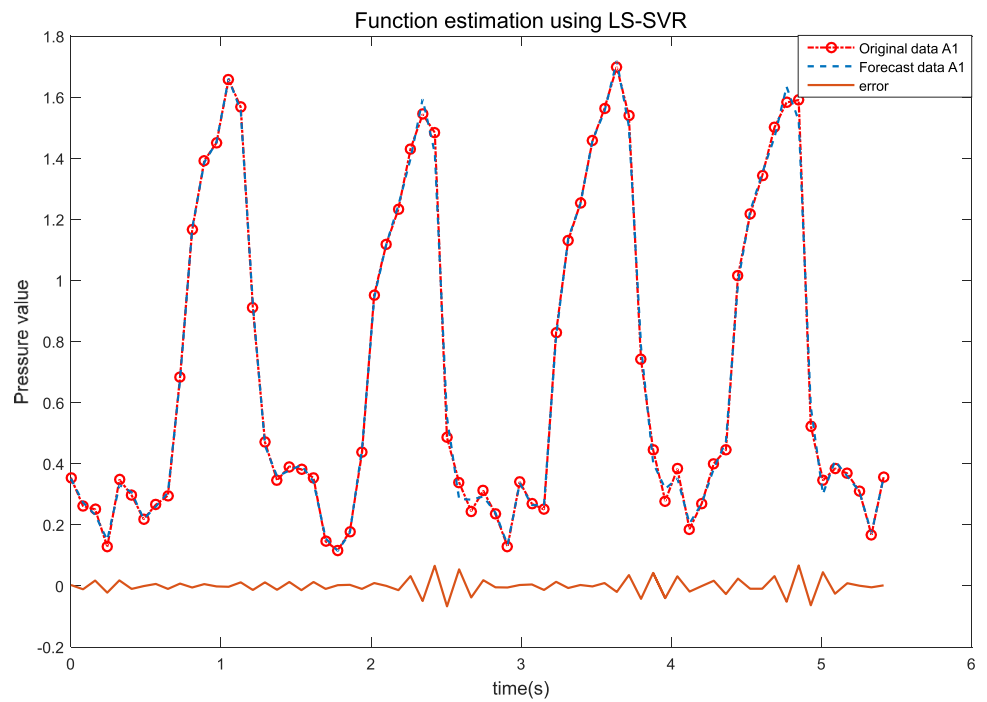
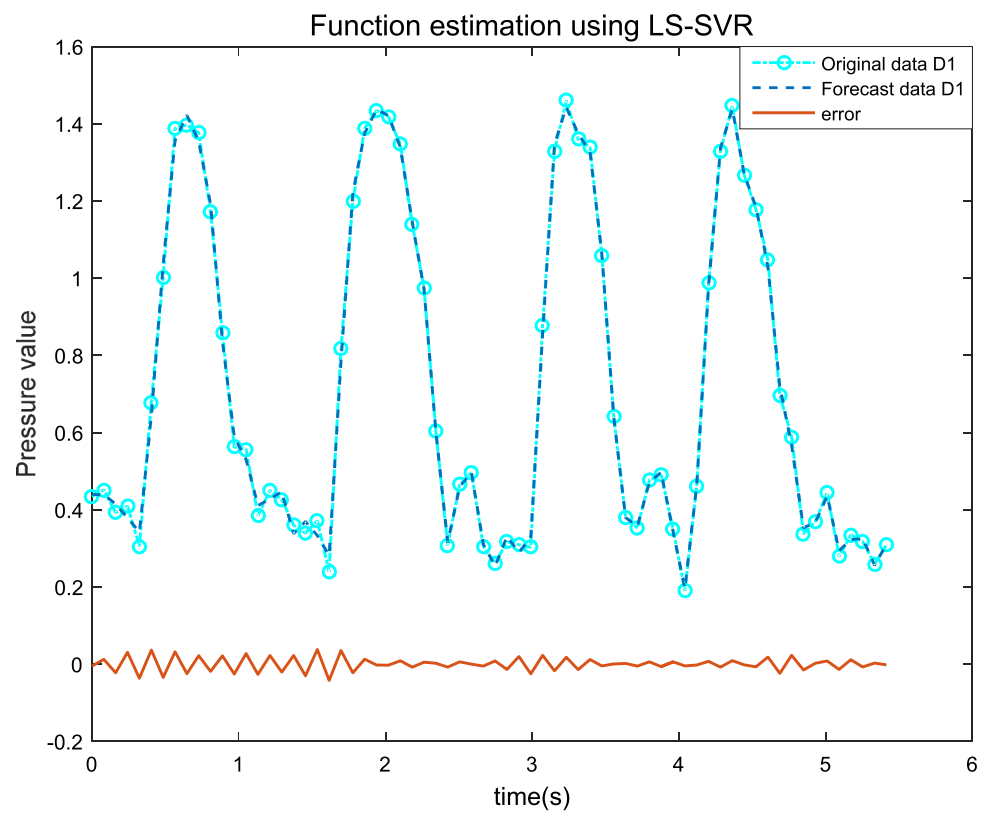**Fig. 7** B_1 prediction of sensor sample data
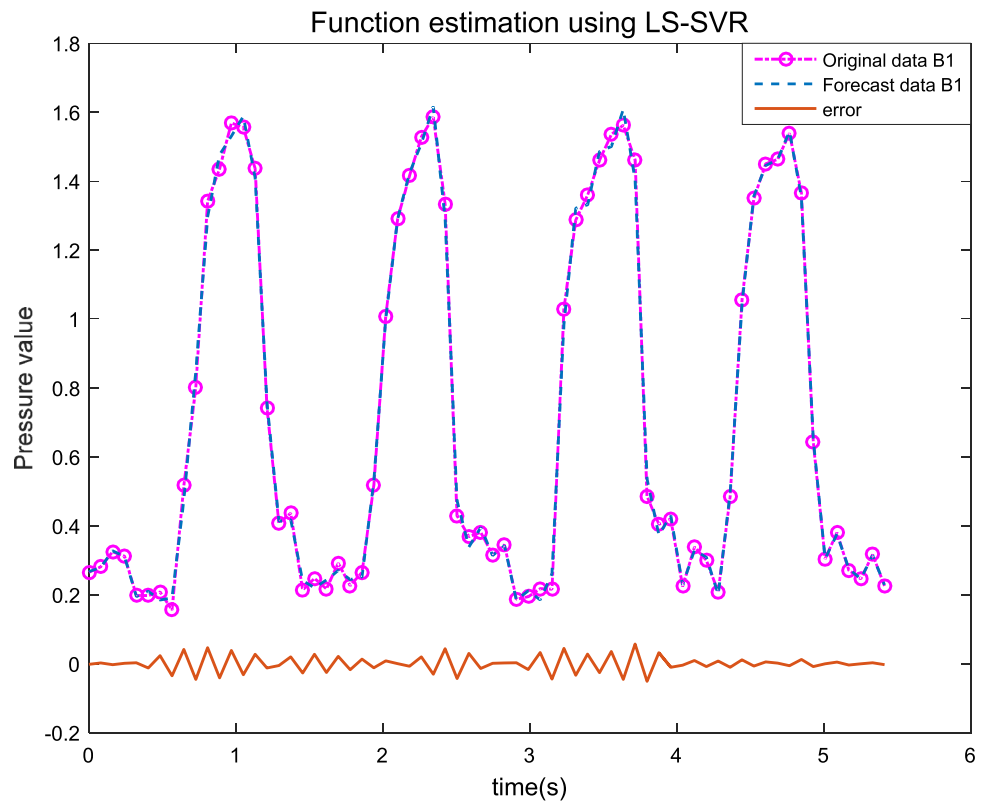
phase, "3" stands for the pre-swing phase, and "4" stands for the swing phase. In a complete gait cycle, the four gait phases of the heel landing phase, the load-supporting phase, the pre-swing phase and the swing phase are perceived at least once, respectively, and recognition is successful. Figures 3 and 2 show four complete cycle gait phase prediction diagrams. "Forecast gait" stands for predicted gait phase curves. "Original Gait" stands for original gait phase curves.

Fig. 8 C_1 prediction of sensor sample data

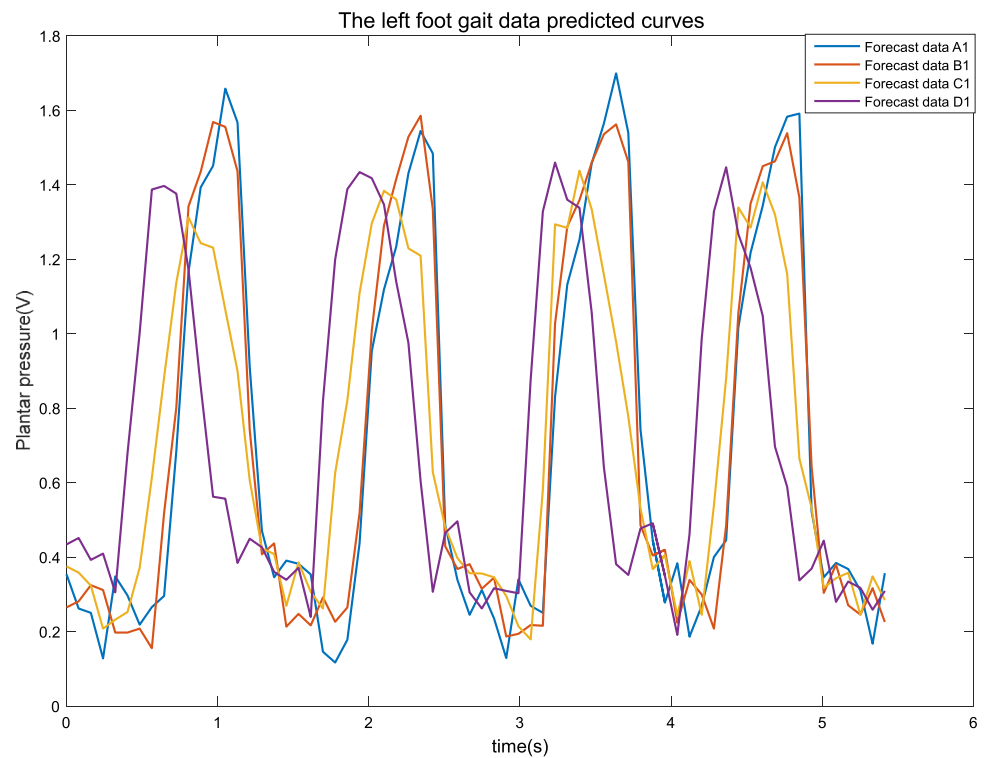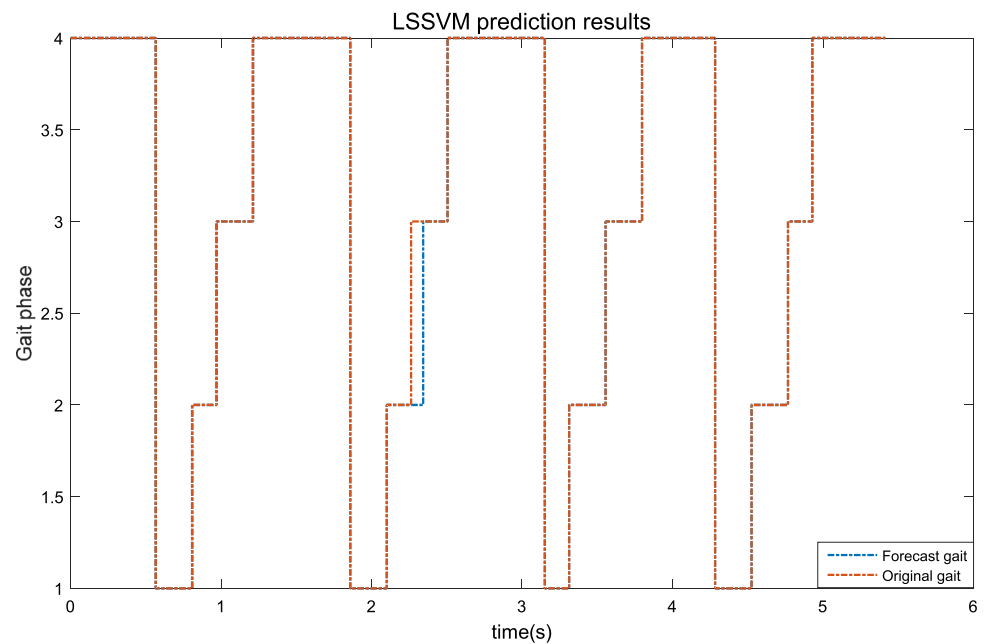**Fig. 9** D_1 prediction of sensor sample data

Fig. 10 Prediction result of sensors sample data

Fig. 11 Human gait phase prediction

Figure 10 shows that four gait phases appear in turn and make periodic changes. In a complete gait cycle, the time proportion of the swing phase is the largest. Predicted gait phase at the same time is the same as the original gait phase. At 2.2642 s, the original gait phase is the pre-swing phase, the predicted gait phase is the load-supporting phase, and the predicted value is wrong. There are two main reasons for this mistake. There is a certain deviation between the gait data predicted by least-squares support vector regression and the real gait data, which leads to a certain error between the predicted gait phase and the actual gait phase. In addition, in selecting *pinv* parameter by experience, the precision of *pinv* parameter selection is missing.

A gait phase recognition algorithm based on fuzzy theory is proposed to recognize 120 predicted gait cycle data in this section. A total of 7200 gait phases are successfully

identified. There are five gait phase recognition errors, including three pre-swing gait phases and two swing gait phases. Moreover, the gait phase recognition rate of predicted gait data is 99.93%.

5.3 Comparing with Kalman prediction algorithm

To verify the effectiveness and accuracy of the proposed algorithm, we choose the Kalman gait prediction algorithm as a comparison to predict the gait stages. Figure 12 shows the recognition results based on Kalman's gait phase prediction algorithm.

Figure 12 indicates gait phase recognition results based on the fusion algorithm of Kalman algorithm and fuzzy theory. The blue line represents the predicted gait phases for the four complete gait cycles. We utilized the same sample set that include 7200 gait phases. Gait phases were recognized only 5824 and the the identification accuracy was 81.08%. By comparing Fig. 11 with Fig. 12, the recognition results of the gait phase recognition algorithm proposed in this paper are outstanding than those based on the algorithm of Kalman gait phase prediction.

6 Conclusion

Based on the sample data of 120 complete gait cycles, a gait data prediction model based on least-squares support vector regression is proposed. The advantage of gait data prediction is that it has a small amount of calculation and high prediction accuracy for small sample data, which has an advantage of real-time gait prediction. The proposed gait data prediction algorithm learns characteristics of sample data and obtains the optimal model. The average accuracy of gait prediction based on least square support vector regression is 99.83%. In addition, a phase recognition algorithm based on fuzzy theory is proposed to recognize the predicted gait data. We design a fuzzy rule table based on gait phase analysis and accomplish fuzzy rule reasoning. The gait recognition rate of the predicted gait data is 99.93%. In order to fully prove the effectiveness of the proposed method, we choose the Kalman gait prediction algorithm for comparison. By analysis of results, the proposed algorithms have outstanding performance.

The algorithms proposed in this paper solve the current exoskeleton sensing technology problem. The lower extremity assisted exoskeleton robot's motion state lags that of the human body due to time delay. The main reason is the lag of gait recognition and transmission in the lower limb exoskeleton assisted robot perception system. Simultaneously, the new method improves the stability and robustness of the lower extremity assisted exoskeleton robot control system. It makes the motion coupling between the exoskeleton system and human lower limbs better and improves the exoskeleton system's comfort and experience.

More attention will be focused on the human lower limb gait perception system based on multi-sensors fusion technology in the following research work. The gait information

Fig. 12 Gait phase prediction of Kalman algorithm
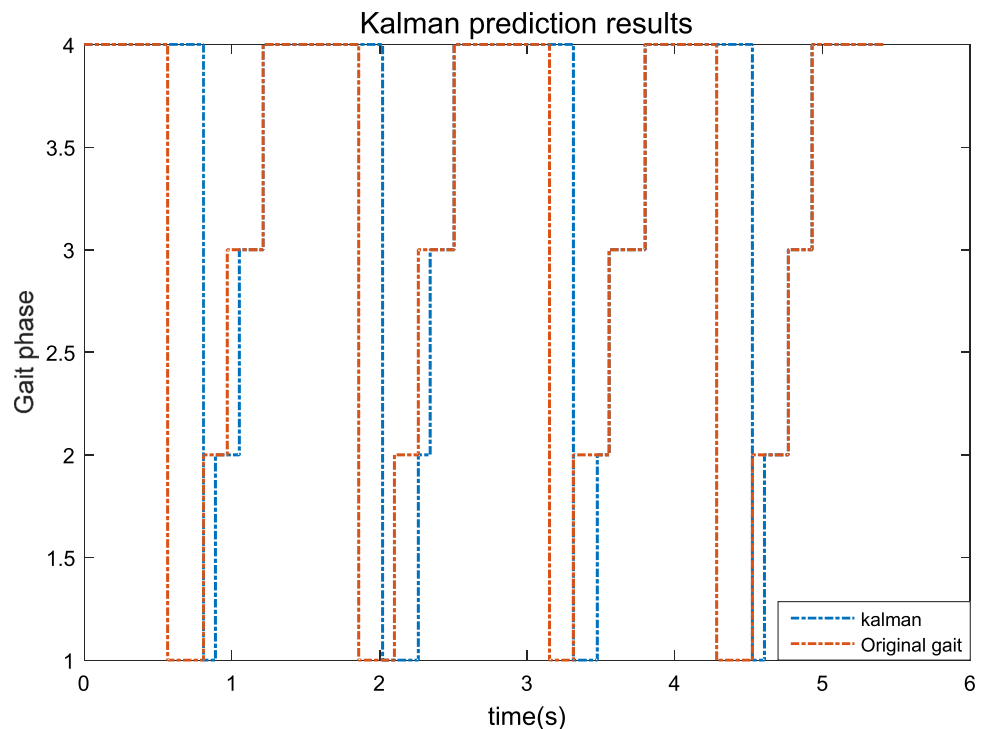
of human lower limbs in different motion states is collected more comprehensively. The precision and efficiency of human gait recognition are realized by combining artificial intelligence decision algorithms.

References

1. Mcgrath RL, Ziegler ML, Piresfernandes M et al (2019) The effect of stride length on lower extremity joint kinetics at various gait speeds. PLOS ONE 14(2):e0200862

2. Ding S, Ouyang X, Liu T et al (2018) Gait event detection of a lower extremity exoskeleton robot by an intelligent IMU[J]. IEEE Sens J 18(23):9728–9735

3. Chia Bejarano N, Ambrosini E, Pedrocchi A, Ferrigno G, Monticone M, Ferrante S (2015) A novel adaptive, real-time algorithm to detect gait events from wearable sensors. IEEE Trans Neural Syst Rehabilit Eng 23(3):413–422

4. Luo J, Tjahjadi T (2020) Gait recognition and understanding based on hierarchical temporal memory using 3D gait semantic folding. Sensors 20:1646

5. Davarzani S, Saucier D, Peranich P, Carroll W, Turner A, Parker E, Middleton C, Nguyen P, Robertson P, Smith B, Ball J, Burch R, Chander H, Knight A, Prabhu R, Luczak T (2020) Closing the wearable gap-part VI: human gait recognition using deep learning methodologies. Electronics 9:796

6. Lishani AO, Boubchir L, Khalifa E et al (2019) Human gait recognition using GEI-based local multi-scale feature descriptors. Multimed Tools Appl 78:5715–5730

7. Akhil VM, Ashmi M, Rajendrakumar PK et al (2020) Human gait recognition using hip, knee and ankle joint ratios. IRBM 41(3):133–140

8. Leclair J, Pardoel S, Helal A et al (2020) Development of an unpowered ankle exoskeleton for walking assist[J]. Disabil Rehabil Assist Technol 15(1):1–13

9. Madden JD (2007) Mobile robots: motor challenges and materials solutions [J]. Science 318(5853):1094–1097

10. Nolan KJ, Ehrenberg N, Kesten AG, et al. (2018) Robotic exoskeleton gait training for inpatient rehabilitation in a young adult with traumatic brain injury[C]. In: *International Conference of the IEEE Engineering in Medicine and Biology Society*, pp. 2809–2812

11. Yuan P, Wang T, Ma F, Gong M (2014) Key technologies and prospects of individual combat exoskeleton[M]. In: Sun F, Li T, Li H (eds) Knowledge engineering and management. Springer, Berlin

12. Mohammadpour R, Shaharuddin S, Chang CK, Zakaria NA, Ab Ghani A, Chan NW (2015) Prediction of water quality index in constructed wetlands using support vector machine. Environ Sci Pollut Res 22(8):6208–6219

13. S Zhu, C Xu, J Wang, Y Xiao and F Ma (2017) Research and application of combined kernel SVM in dynamic voiceprint password authentication system. In: *2017 IEEE 9th International Conference on Communication Software and Networks (ICCSN)*, Guangzhou, China, pp. 1052–1055

14. Yunlong Z, Peng Z (2012) Vibration fault diagnosis method of centrifugal pump based on EMD complexity feature and least square support vector machine[J]. Energy Procedia 17:939–945

15. Almasi ON, Khooban MH, Behzad H (2018) Non-linear MIMO identification of a Phantom Omni using LS-SVR with a hybrid model selection. IET Sci Meas Technol 12(5):678–683

16. Mesquita DPP, Freitas LA, Gomes JPP, Mattos CLC (2020) LS-SVR as a Bayesian RBF network. EEE Trans Neural Netw Learn Syst 31(10):4389–4393

17. LopezMeyer P, Fulk GD, Sazonov ES (2011) Automatic detection of temporal gait parameters in poststroke individuals. IEEE Trans Inf Technol Biomed 15(4):594–601

18. Liao R, Yu S, An W, Huang Y (2020) A model-based gait recognition method with body pose and human prior knowledge. Pattern Recognit. 98:107069

19. Ben X, Gong C, Zhang P et al (2020) Coupled bilinear discriminant projection for cross-view gait recognition[J]. IEEE Trans Circuits Syst Video Technol 30(3):734–747

20. MS Ivanova, (2019) Fuzzy set theory and fuzzy logic for activities automation in engineering education. In: *2019 IEEE XXVIII International Scientific Conference Electronics (ET)*, Sozopol, Bulgaria, pp. 1-4

21. Kumar PS (2020) Algorithms for solving the optimization problems using fuzzy and intuitionistic fuzzy set[J]. Int J Syst Assur Eng Manag 11(1):189–222

22. VSR Poli, (2017) A method for generalized fuzzy rough sets and application to fuzzy control systems. In: *2017 International Conference on Fuzzy Theory and Its Applications (iFUZZY)*, Pingtung, pp.1–6

23. Zhang Y, Ansari N, Su W, et al. (2011) Multi-sensor signal fusion based modulation classification by using wireless sensor networks[C]. International conference on communications, pp. 1–5

24. J Yang, A Bouzerdoum and SLPhung, (2010) A training algorithm for sparse LS-SVM using compressive sampling. In: *2010 IEEE International Conference on Acoustics, Speech and Signal Processing*, Dallas, TX, pp. 2054–2057